4.1

NITRIC ACID “RENOXIFICATION” IN THE TROPOSPHERE: FROM A MODELING MYTH TO A LABORATORY REALITY

Armando M. Rivera-Figueroa and Barbara J. Finlayson-Pitts*
Department of Chemistry, University of California, Irvine
Irvine, CA 92697-2025

ABSTRACT

The partitioning of nitrogen oxides in the atmosphere, in particular the NO_x/HNO_3 ratio, has not historically been accurately reproduced by models. Although the model under-prediction of the NO_x/HNO_3 ratio has been improved by the new rate constants for the reactions of OH with NO_2 and HNO_3, the discrepancy between the field and modeled ratios has not been clearly resolved. Heterogeneous reactions of HNO_3 with various atmospheric gaseous species, including NO, CO, CH_4, and SO_2, have been proposed to reconcile these ratios. We present laboratory studies in which the possibility of heterogeneous reactions between HNO_3 adsorbed on silica surfaces and gaseous NO, CO, CH_4, and SO_2 were investigated. Two different silica surfaces, a porous glass plate and pressed silica (Cab-O-Sil®) pellets, were used as substrates for HNO_3. Both the gas phase and the surface species were monitored with time using FTIR at 1 atm total pressure in N_2 and 298 K. No reaction was observed between $HNO_{3(ads)}$ and CO, CH_4 or SO_2, from which upper limits for the reaction probabilities (γ^{rxn}) were derived: γ^{CO} and $\gamma^{SO2} \leq 10^{-10}$, and $\gamma^{CH4} \leq 10^{-12}$. The effect of Fe^{3+} and H_2SO_4 on the reaction with CO was also investigated, and no enhancement of the reaction was observed under either of these conditions. Nitric oxide does react with the undissociated form of HNO_3 adsorbed on the silica pellets, but not the anion NO_3^-, to form NO_2 and a water-nitric acid complex. A lower limit for the reaction probability of gaseous NO with HNO_3 adsorbed on silica pellets was calculated: $\gamma^{NO} = (6 \pm 2) \times 10^{-9}$ (2s). The atmospheric implications of HNO_3 “renoxification” on common surfaces will be discussed.

INTRODUCTION

In major urban areas, the primary pollutants include nitrogen oxides ($NO_x = NO + NO_2$) and volatile organic compounds (VOC’s), which undergo photochemical reactions to produce ozone (O_3) and nitric acid (HNO_3) in the troposphere among others. Nitric acid may undergo various reactions in the troposphere, as shown schematically in Figure I, including the possible recycling of NO_x.

Many of the key parameters required to estimate the influence of NO_x in the chemistry of the atmosphere remain uncertain. Thus, understanding of the concentration, distribution and interaction of NO_x with other species in the atmosphere, its sources and sinks, is extremely important. While NO_x chemistry has been the focus of a number of studies [*Finlayson-Pitts and Pitts*, 2000], the partitioning of nitrogen in the atmosphere, in particular the NO_x/HNO_3 ratio, has generally not been accurately reproduced by models [*Chatfield*, 1994; *Singh et al.*, 1998; *Gao et al.*, 1999; *Lary and Shallcross*, 2000; *Perkins et al.*, 2001]. For example, in 1998 the World Meteorological Organization concluded that below 30 km in the atmosphere (troposphere and lower stratosphere), measured NO_2/NO and NO_2/HNO_3 ratios are greater than those calculated by models which include known gas phase nitrogen reactions relevant to the troposphere [*WMO*, 1998]. Gao *et al.* (1999) and Perkins *et al.* (2001) reported that the use of revised values of the rate constants for the reaction of OH with NO_2 [*Brown et al.*, 1999a; *Dransfield et al.*, 1999] and with HNO_3 [*Brown et al.*, 1999b] improves the agreement between the measured and modeled values in the lower stratosphere, but it is still not clear whether unknown chemistry affects the measured ratio. Therefore, heterogeneous reactions of HNO_3 have been proposed as a possible source of this discrepancy between models and atmospheric measurements [*Fairbrother et al.*, 1997; *Lary and Shallcross*, 2000].

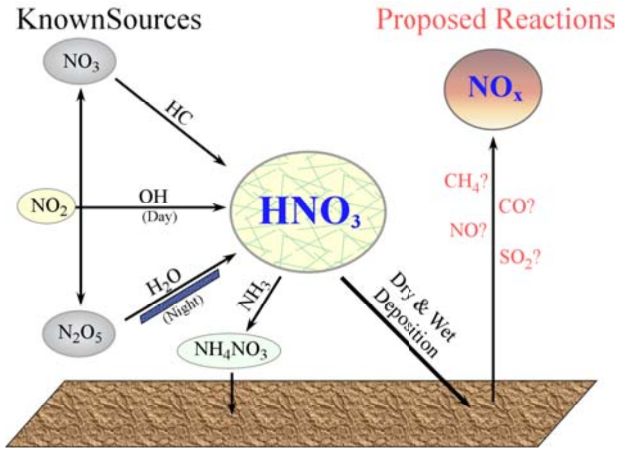

Figure I: HNO_3 reaction pathways in the troposphere.

Corresponding author: Barbara J. Finlayson-Pitts, University of California, Irvine, Dept of Chemistry, Irvine, CA 92697-2025; e-mail: bjfinlay@uci.edu

As illustrated in Figure I, NO_x is converted to HNO_3 and then removed from the atmosphere primarily by wet or dry deposition. Nitric acid may also be removed from the atmosphere through reaction with ammonia (NH_3):

$$NH_3 + HNO_3 \leftrightarrow NH_4NO_{3\,(s,\,aq)} \tag{1}$$

Ammonium nitrate (NH_4NO_3), which may also undergo dry or wet deposition, is an important component of atmospheric particulate matter in polluted atmospheres [*Finlayson-Pitts and Pitts*, 2000; *Hughes et al.*, 2000]. As a result, the formation of HNO_3 is generally considered to result in the permanent removal of NO_x from the atmosphere.

Surfaces present in the atmosphere, however, can catalyze certain chemical reactions that would otherwise be kinetically and thermodynamically unfavorable in the gas phase. In order to understand the atmospheric NO_x cycle, it is important to study possible candidates for surface reactions that are not currently considered by models. Since the lower portion of the troposphere contains appreciable amounts of surfaces, such as pavement, asphalt, buildings, plants and atmospheric aerosols, it is of interest to investigate the possible heterogeneous reactions that may occur on these surfaces or model substrates for them.

Gaseous species, such as methane (CH_4), sulfur dioxide (SO_2), carbon monoxide (CO) and NO, have been proposed as possible candidates to react with surface adsorbed HNO3 [*Fairbrother et al.*, 1997]. On the basis of their thermodynamic characteristics, Fairbrother *et al.* (1997) have suggested the following:

$$HNO_3 + NO \xrightarrow{surface} HONO + NO_2 \tag{2}$$

$$HNO_3 + CO \xrightarrow{surface} HONO + CO_2 \tag{3}$$

$$HNO_3 + SO_2 + H_2O \xrightarrow{surface} HONO + H_2SO_4 \tag{4}$$

$$2\,HNO_3 + CH_4 \xrightarrow{surface} 2\,HONO + H_2CO + H_2O \tag{5}$$

If these heterogeneous reactions occur, they may represent pathways for HNO_3 to be transformed back to reactive gaseous compounds, *e.g.* NO, NO_2 and HONO. This process is what has been called “renoxification”. The deposition of HNO_3 to surfaces thus would become an “active” part of a cycle in NO_x chemistry, rather than a permanent sink. Therefore, these pathways will be important when simulating the NO_x/HNO_3 ratio measured in the atmosphere.

More recently, Lary and Shallcross (2000) have shown by modeling studies that if the reaction probability of CO with HNO_3, reaction (6), is $\gamma \geq 2 \times 10^{-4}$, the agreement between the measured and modeled NO_x/HNO_3 ratio in the upper troposphere would improve significantly.

As mentioned above, reactions (2) – (5) can produce nitrous acid (HONO) in the atmosphere, which is photodissociated by ultraviolet radiation ($\lambda < 400$ nm) to produce NO and OH. The OH radical initiates chain reactions by attacking VOC’s and other species in the atmosphere [*Finlayson-Pitts and Pitts*, 2000]. Therefore, gaseous HONO plays an important role in the chemistry of irradiated mixtures of VOC’s and NO_x in air, having direct and indirect impacts on photochemical smog formation, including environmental and human health problems [*Finlayson-Pitts and Pitts*, 2000].

Previously, Finlayson-Pitts and coworkers have studied the reaction of NO with HNO_3 on a high surface area porous glass, reaction (2) [*Mochida and Finlayson-Pitts*, 2000]. They also evaluated the effect of the variation of relative humidity on the reaction at much lower NO concentrations using smooth borosilicate glass [*Saliba et al.*, 2000; *Saliba et al.*, 2001]. This reaction, producing gaseous NO_2 and HONO, was observed to be much faster with ~3 monolayers of water.

Here, we report FTIR studies of reactions (2) – (5). A pressed silica pellet was used in addition to porous glass in order to probe for the effects of the underlying surface. Also, the possible catalysis by Fe^{3+} proposed by Lary and Shallcross (2000), and effects of H_2SO_4 on the surface were investigated for reaction (3). The atmospheric implications are discussed.

EXPERIMENTAL

A Fourier transform infrared spectrometer (FTIR) (Mattson Research Series) was used to characterize both the species adsorbed on the surface and in the gas phase, and to monitor their change with time. The spectra were collected using 32 co-added scans at a resolution of 1 cm^{-1}.

The reaction cell, shown in Figure II, is made of borosilicate glass and has ZnSe windows [*Barney and Finlayson-Pitts*, 2000]. The cell has a volume of 79 cm^3, a geometric surface area of 232 cm^2, and a pathlength of 6.3 cm. The surface used for the reaction is suspended on a borosilicate glass holder in the center of the cell. This holder allows the movement of the surface in and out of the infrared beam, permitting both the characterization of the surface and the gas phase during the reaction.

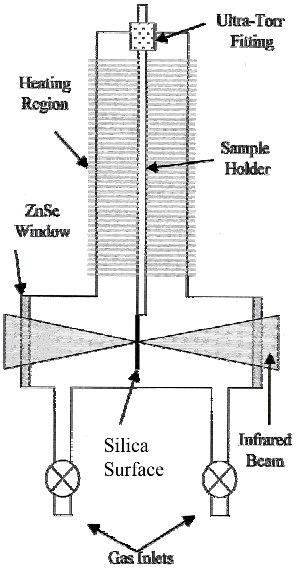

Figure II: FTIR reaction cell schematic.

A typical experiment consists of first heating the reaction cell up to ~320 °C while pumping in order to remove some of the adsorbed water. Nitric acid was introduced into the reaction cell several times (~1 × 10^{17} molecule cm^{-3}), and then pumped for about 30 minutes to remove gaseous HNO_3. Subsequently, the reactant gases were introduced and the reaction progress monitored using FTIR over time.

In order to monitor the reaction progress, and be able to distinguish between surface-adsorbed species and gas phase species using FTIR, absorption spectra were obtained as shown schematically in Figure III. First, the absorption spectrum of the gas plus adsorbed species and of the gaseous species only were obtained, Figure IIIA and IIIB, respectively. Then the spectrum of Figure IIIB was subtracted from the spectrum of Figure IIIA to obtain the spectrum of species adsorbed on the surface, Figure IIIC.

The surface area was measured using an Accelerated Surface Area and Porosimetry System (ASAP 2000, Micromeritics). The measurement is based on the Brunauer-Emmett-Teller (BET) method using nitrogen (N_2) as the adsorbate [*Brunauer et al.*, 1938].

In separate studies, ion chromatography (IC) (Alltech Odyssey) was used in order to quantify the HNO_3 adsorbed on the surfaces. After the silica surface was dosed with HNO_3 the pellet was removed from the cell, rinsed with nanopure water and this water analyzed then for the nitrate anion (NO_3^-). The IC was calibrated for NO_3^- using aqueous solutions prepared from sodium nitrate powder.

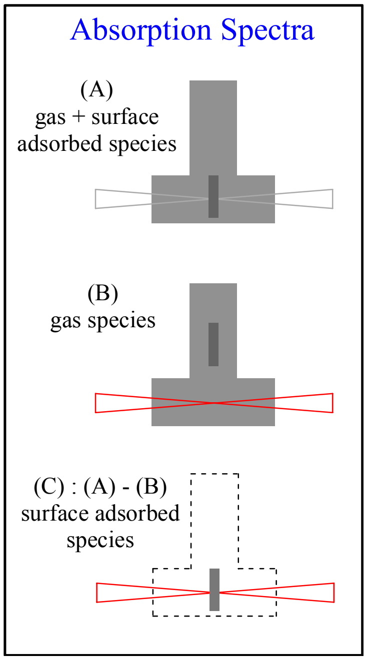

Figure III: Procedure to follow in order to obtain the absorption spectrum of both the gas phase and the surface-adsorbed species.

SILICA SURFACES

Silica is ubiquitous among construction materials, and therefore in urban, remote and pristine areas as well, where it is present in its natural forms, *e.g.* sand, quartz, etc. Table 1 shows the percentage by weight of silica in some construction materials of relevance [*Association*, 1999; *BNZ Materials*, 1999a,b; *USGS*, 1999].

Two different types of silica surfaces, porous glass plate (Corning) and pressed silica (Cab-O-Sil®) pellet, were used. The porous glass is about 1 mm thick and has been etched in the center to a thickness of approximately 0.3 mm by submerging it in a 7.7% (v:v) hydrofluoric acid (HF) solution for 21 minutes [*Barney and Finlayson-Pitts*, 2000]. The chemical composition of porous glass is 96.3% of SiO_2, 2.95% of B_2O_3, 0.04% of Na_2O and 0.72% of Al_2O_3 + ZrO2 [*Elmer*, 1992], with a total surface area of 71.2 m^2/g. The surface dimensions are 2 cm wide by 3 cm height and its weight is 0.40 g resulting in a total surface area of 28.5 m^2. The surface was cleaned either by heating in an oven to about 500 °C, causing desorption of the organic compounds, or by boiling in a peroxide (H_2O_2) solution (70%) at about 95 °C, then washing the surface several times with deionized water and drying it in an oven at about 150 °C [*Elmer*, 1992].

Table 1: Contents by weight percentage of some common surface materials.

Material	Composition
Sediment	sand, silt, and clay (particle diameter of 2 mm – 0.002 mm) > 98% crystalline quartz (SiO_2) (SiO_2 percentage depends on the surrounding environment)
Cement	50% $3CaO \cdot SiO_2$ + 25% $2CaO \cdot SiO_2$ + 10% $3CaO \cdot Al_2O_3$ + 10% $4CaO \cdot Al_2O_3 \cdot Fe_2O_3$ + 5% $CaSO_4 \cdot 2H_2O$
Concrete	water + cement + aggregate (sand, crushed limestone, etc) (The percentage of cement and aggregate varies with the desired properties of the concrete) (Known as mortar when the aggregate used is sand)
Asphalt	95% aggregate of sand, stone or gravel + 5% asphalt cement (product of crude oil)
Bricks	Insulating fire brick – 0.1% to 40% SiO_2 Silica brick - 95% SiO_2

Other experiments were performed using pressed silica (Cab-O-Sil®) pellets as the surface. Cab-O-Sil® is an untreated fine fumed silica powder (particles with a size range of 10 to 20 Å) of high purity with a chemical composition of more than 99.8% of SiO_2 [*CABOT*, 1999]. This silica powder, with a surface area of 329.1 m^2/g, is commercially available and can be easily compressed into a pellet. Most Cab-O-Sil® pellets were formed using an evacuable pellet dye (Specac®) charged with approximately 0.02 g of Cab-O-Sil® powder and a pellet press (Carver Laboratories Inc., Model C). The resulting pellet has a diameter of 13 mm, a thickness of approximately 0.1 to 0.5 mm and an approximate total surface area of 6.5 m^2. Thickness varies with the quantity of sample charged in the dye and pressure applied to the sample.

These surfaces differ from each other in terms of their infrared absorption spectra [*Kiselev and Lygin*, 1975] and surface area. As shown in Figure IV, the porous glass and Cab-O-Sil® absorb infrared radiation efficiently below 1500 and 1300 cm^{-1}, respectively.

Silica surfaces have several characteristic infrared bands. Single or "free" surface silanol (Si-OH) groups at 3742 cm^{-1} generate some of these bands. A broad band at 2800 – 3800 cm^{-1} is generated by the combination of the hydrogen-bonded silanol groups (3550 cm^{-1}), perturbed silanol groups by interparticle contact (3650 cm^{-1}) and liquid water. In addition, the silica skeleton vibration band can be seen in the region from 1300 – 2000 cm^{-1} [*Low and Ramasubramanian*, 1966; *Papirer*, 2000].

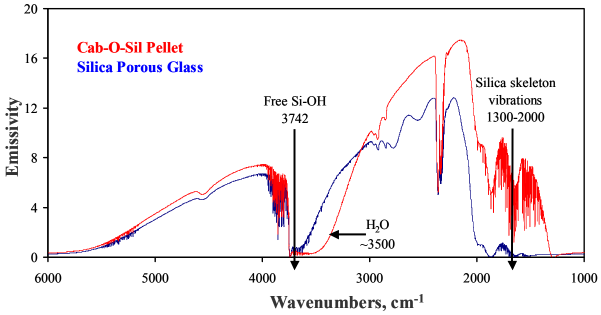

Figure IV: Infrared transmission of silica surfaces.

RESULTS AND DISCUSSION

Reactions (2) – (5) have been studied on both types of surfaces, porous glass plate and pressed silica pellets, under ambient conditions (25 °C, 1 atm). The total nitrate (= HNO_3 + NO_3^-) adsorbed on the surface, measured by IC, was ~2.5 × 10^{18} molecules, resulting in ~4 × 10^{13} molecule cm^{-2} for the pressed silica pellet.

The reaction between $HNO_{3(ads)}$ and CO, reaction (3), was studied using CO concentrations ranging from (3 – 26) × 10^{16} molecule cm^{-3}. No reaction was observed even after a period of one hour for the porous glass plate and two hours on the pressed silica pellet. The effect of Fe^{3+} was also examined using a pressed pellet prepared from a mixture of silica:$FeCl_3$ (10:1 w:w). No catalytic effect of Fe^{3+} was observed. Also, the effect of the presence of H_2SO_4 on the reaction was examined by submerging a previously prepared press silica pellet in concentrated H_2SO_4. No enhancement of the reaction was observed due to H_2SO_4.

For reaction (4), the concentrations of SO_2 used ranged from (5 – 18) × 10^{16} molecule cm^{-3}. No reaction between $HNO_{3(ads)}$ and SO_2 was observed, under dry or humid conditions, *e.g.* 40% RH, even after a period of two hours on either silica surface. Gas phase SO_2 was also monitored for a period of three hours using the characteristic bands at 1360 and 1152 cm^{-1} and no decrease was observed.

Reaction (5) was studied using CH_4 concentrations ranging from (1 – 19) × 10^{16} molecule cm^{-3}. No reaction between $HNO_{3(ads)}$ and CH_4 was observed even after a period of two hours on either of the two silica surfaces.

The heterogeneous reaction of NO with $HNO_{3(ads)}$, reaction (5), was studied using NO concentrations ranging from (2 – 14) × 10^{16} molecule cm^{-3}. As shown in Figure V and VI, exposure of $HNO_{3(ads)}$ to NO led to the disappearance of HNO_3 bands at 1313 cm^{-1}, 1400 cm^{-1}, 1677 cm^{-1}, 2735 cm^{-1}, and 2970 cm^{-1}, as well as the NO band at 1876 cm^{-1} (not shown). Product peaks were observed at 1617 cm^{-1} (NO_2) and 1745 cm^{-1} (N_2O_4). Also, a broad band was observed peaking around 3300 cm^{-1}. Figure VIIb, which is the spectrum obtained after subtracting the remaining $HNO_{3(ads)}$ and NO_2, shows a band at 1640 cm^{-1}.

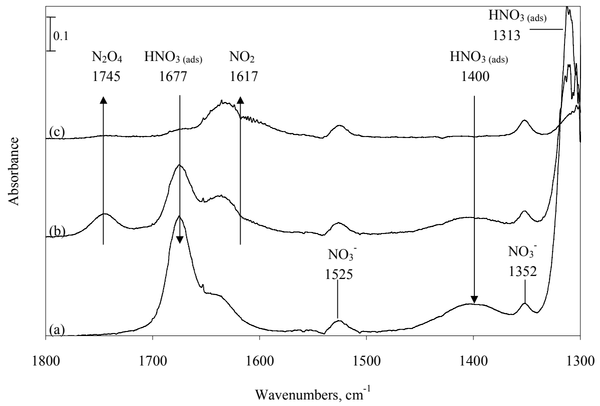

Figure V: (a) Spectrum of the gas phase plus surface adsorbed HNO_3 on silica in the 1300-1800 cm^{-1} region; (b) immediately after the introduction of 9.7×10^{16} NO cm^{-3}, and (c) 65 minutes later.

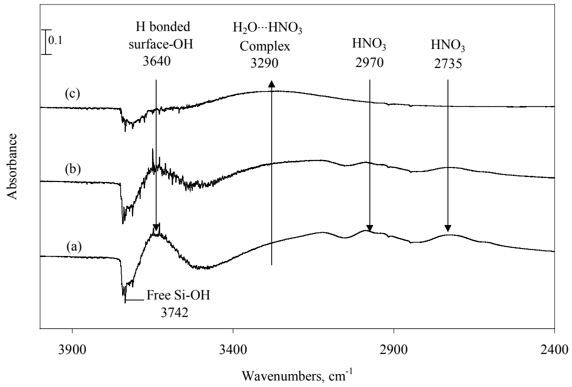

Figure VI: Spectra of the gas plus surface in the 2400 – 3900 cm^{-1} region. Spectra (a), (b), and (c) correspond to those in Figure V.

Ab initio calculations suggest that red-shifts of ~300 – 500 cm^{-1} in the OH stretching frequency of HNO_3 are caused by the formation of a H_2O-HNO_3 complex [*Staikova and Donaldson*, 2001; *Tao et al.*, 1996]. Furthermore, in recent *ab initio* studies, McCurdy *et al.* (2002) have shown that the formation of a 1:1 complex of $H_2O\bullet HNO_3$ results in a red-shift in the OH stretching frequency of HNO_3 by 420 cm^{-1}, showing a peak at around 3300 cm^{-1} [*McCurdy et al.*, 2002]. Only small shifts were observed for the water band around 1600 cm^{-1} (ν_2 bend) [*Tao et al.*, 1996; *Staikova and Donaldson*, 2001; *McCurdy et al.*, 2002]. Although these *ab initio* studies represent interactions typical of the gas phase, the relative magnitudes of the observed shifts in these two bands in our experiments suggest that the peaks observed at ~3300 cm^{-1} and 1640 cm^{-1} are due to the formation of a H_2O-HNO_3 complex.

In addition, the peak heights of the bands due to NO_3^- at 1352 cm^{-1} and 1525 cm^{-1} do not change significantly (Figure V), suggesting that the dissociated form of HNO_3 does not play a role in the "renoxification" process observed for reaction (2). Previous work of Rivera-Figueroa *et al.* (2002) shows that reaction (2) does not occur with surface adsorbed NH_4NO_3, confirming the suggestion that the undissociated form of HNO_3 is necessary for reaction (2) to occur.

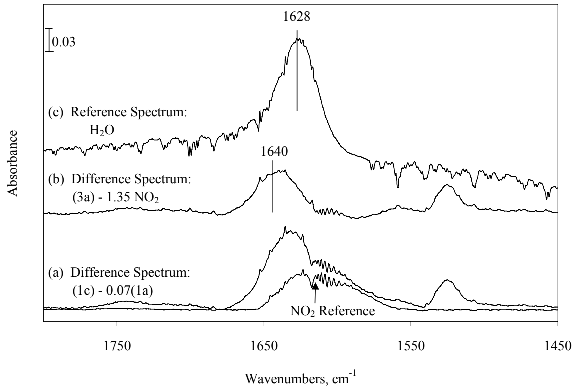

Figure VII: (a) Spectrum after 65 minutes of reaction (Figure Vc) after subtraction of adsorbed HNO_3 ($0.07 \times$ initial spectrum, Figure Va); also shown is a reference spectrum of gas phase NO_2 (3.2×10^{16} molecule cm^{-3}) (b) Difference spectrum after subtraction of gaseous NO_2 ($1.35 \times$ reference spectrum in Fig. VIIa) from spectrum in (a); (c) Reference spectrum of water adsorbed on silica pellet.

Mochida and Finlayson-Pitts (2000) proposed a pathway for the reaction of NO with $HNO_{3(ads)}$ on silica glass, in which HONO is an intermediate [*Mochida and Finlayson-Pitts*, 2000]:

$$NO_{(g)} + HNO_{3(ads)} \xrightarrow{surface} NO_{2(g)} + HONO_{(ads)} \quad (6)$$

$$HONO_{(ads)} + HNO_{3(ads)} \xrightarrow{surface} N_2O_{4(ads)} + H_2O_{(l)} \quad (7)$$

$$N_2O_{4(ads)} \xleftrightarrow{surface} 2\ NO_{2(g)} \quad (8)$$

Therefore, the net NO_x production that may contribute to "renoxification" in the atmosphere is given by the net reaction (9):

$$NO_{(g)} + 2\ HNO_{3(ads)} \xrightarrow{surface} 3\ NO_2 + H_2O \qquad (9)$$

Figure VIII shows a schematic of reaction (2) in which water is present in the system. Here, adsorption of HNO_3 on the Si-OH groups occurs followed by the displacement of the HNO_3 by water and the reaction of NO with $HNO_{3(ads)}$.

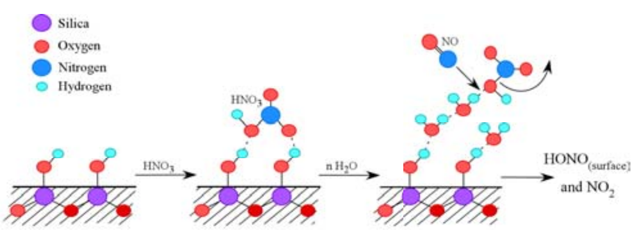

Figure VIII: Schematic of proposed reaction mechanism for reaction (2).

Reaction Probability Calculations

Upper limits to the reaction probabilities for the different gaseous species (G = CO, CH_4 or SO_2) reacting with surface-adsorbed HNO_3 were calculated using the initial rate of loss of the gas G (-d[G]/dt), the cell volume (V_{cell} = 79 cm^3), the surface area (A = 6.5 m^2) of the pressed silica pellet and M, the molecular weight of G:

$$\gamma = \frac{\left(\frac{-d[G]}{dt}\right) \times V_{cell}}{A[G]_o \sqrt{\frac{RT}{2\pi M}}} \qquad \textbf{(I)}$$

Although no reaction was observed for SO_2, CO, and CH_4 reactants, slow losses of these reactants were measured that were not statistically different from their measured losses in a clean cell with no silica surface present. As shown in Figure IX for SO_2, we conducted a least-squares analysis of this loss of [G] versus time to obtain the maximum possible loss of the gas under these experimental conditions, and hence to calculate an upper limit of the value for the reaction probability. We define the maximum loss rate as the lower 95% confidence limit of the slope of [G] versus time. This approach gave upper limits for the reaction probabilities of reactions (3) – (5) of $\gamma^{CO} \leq 10^{-10}$, $\gamma^{CH4} \leq 10^{-12}$ and $\gamma^{SO2} \leq 10^{-10}$.

The upper limit obtained for reaction (3) is six orders of magnitude smaller than the reaction probability used previously by Lary and Shallcross (2000) in their modeling studies. Therefore, reaction (3) jointly with reactions (4) and (5) seem unlikely to be responsible for the discrepancy between the measured and modeled NO_x/HNO_3 ratios, contrary to what has been proposed.

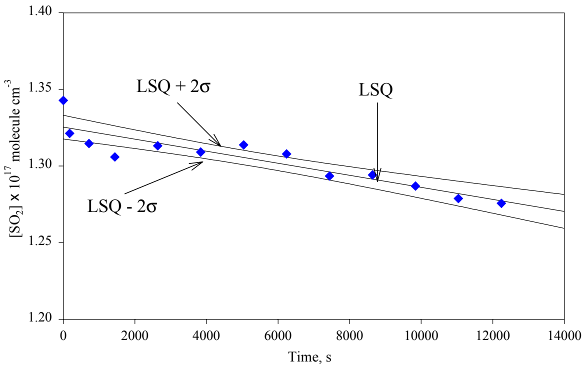

Figure IX: Time dependence of SO_2 in the presence of $HNO_{3(ads)}$. The upper and lower limits (± 2σ) of the linear regression are shown. As discussed in the text, this loss is not statistically different from that in the absence of the silica surface.

For the NO reaction, reaction (2), we followed the lost of HNO_3 with time. We used half of the initial rate of loss of surface-adsorbed HNO_3, based on the stoichiometry of the overall reaction (9), as a measure of d[NO]/dt. The reaction is sufficiently fast that under the conditions of Figure V, ~ 43% of the initial HNO_3 reacts by the time the first spectrum is obtained (2 scans in 2.2 s), *i.e.* an average reaction time of 1.1 s. This change in the HNO_3 concentration leads to a calculated reaction probability of $\gamma^{NO} = 7 \times 10^{-9}$. The reaction probability, calculated for a set of seven experiments, is $\gamma^{NO} = (6 \pm 2) \times 10^{-9}$ (2s), similar to the reaction probability on the order of 10^{-8} estimated by Saliba *et al*. (2001) for reaction (2) on a smooth borosilicate glass surface at 50% RH. However, this value is a lower limit because we were not able to monitor continuously the very fast initial rate of HNO_3 loss.

SUMMARY

This research shows that reactions between $HNO_{3(ads)}$ and CO, CH_4, and SO_2 are not likely to be important in the atmosphere as "renoxification" processes. On the other hand, it also shows that the reaction of NO with $HNO_{3(ads)}$ occurs, demonstrating that surfaces may play a significant role in the chemistry of the atmosphere. This heterogeneous chemistry between NO and adsorbed HNO_3, which depends on relative humidity [*Saliba et al.*, 2001], could contribute to "renoxification" in the atmosphere. The results obtained in this study may help explain the discrepancies in the modeled *versus* observed NO_x/HNO_3 ratios. In addition, modeling studies by Knipping and Dabdub (2002) have shown that including reaction (2) in the airshed model may decrease discrepancies between field measurements and model predictions of ozone.

ACKNOWLEDGEMENTS

We are grateful to the California Air Resources Board (Contract # 00-323) and to the Office of Graduate Studies of the University of California at Irvine, for financial support of this project. We would also like to express our gratitude to J. N. Pitts, Jr. and N. A. Saliba for helpful discussions.

REFERENCES

Barney, W.S., and B.J. Finlayson-Pitts, 2000: Enhancement of N_2O_4 on porous glass at room temperature: A key intermediate in the heterogeneous hydrolysis of NO_2?, *J. Phys. Chem. A*, **104** (2), 171-175.

BNZ Materials, Inc., Insulating Fire Brick - Material Safety Data Sheet, Littleton, CO, 1999a.

BNZ Materials, Inc., Silica Brick and Mortar, Littleton, CO, 1999b.

Brown, S.S., R.K. Talukdar, and A.R. Ravishankara, 1999a: Rate constants for the reaction $OH + NO_2 + M \rightarrow HNO_3 + M$ under atmospheric conditions, *Chem. Phys. Lett.*, **299**, 277-284.

Brown, S.S., R.K. Talukdar, and A.R. Ravishankara, 1999b: Reconsideration of the rate constant for the reaction of hydroxyl radicals with nitric acid, *J. Phys. Chem. A*, **103**, 3031-3037.

Brunauer, S., P.H. Emmett, and E. Teller, 1938: Adsorption of gases in multimolecular layers, *J. Am. Chem. Soc.*, **60**, 309-319.

CABOT, CAB-O-SIL(R) HS-5 Untreated Fumed Silica, CABOT Corporation, Tuscola, IL, 1999.

Chatfield, R.B., 1994: Anomalous HNO_3/NO_x Ratio of Remote Tropospheric Air: Conversion of Nitric Acid to Formic Acid and NO_x?, *Geophys. Res. Lett.*, **21**, 2705-2708.

Dransfield, T.J., K.K. Perkins, N.M. Donahue, J.G. Anderson, M.M. Sprengnether, and K.L. Demerjian, 1999: Temperature and pressure dependent kinetics of the gas-phase reaction of the hydroxyl radical with nitrogen dioxide, *Geophys. Res. Lett.*, **26** (6), 687-690.

Elmer, T.H., Porous and Reconstructed Glasses, in *Engineered Materials Handbook*, pp. 427-432, ASM International, Materials Park, Ohio, 1992.

Fairbrother, D.H., J.D. Sullivan, and H.S. Johnston, 1997: Global thermodynamic atmospheric modeling: Search for new heterogeneous reactions, *J. Phys. Chem. A*, **101**, 7350-7358.

Finlayson-Pitts, B.J., and J.N.J. Pitts, *Chemistry of the Upper and Lower Atmosphere: Theory, Experiments, and Applications*, Academic Press, San Diego, CA, 2000.

Gao, R.S., D.W. Fahey, L.A. Del Negro, S.G. Donnelly, E.R. Keim, J.A. Neuman, E. Teverovskaia, P.O. Wennberg, T.F. Hanisco, E.J. Lanzendorf, M.H. Proffitt, J.J. Margitan, J.C. Wilson, J.W. Elkins, R.M. Stimpfle, R.C. Cohen, C.T. McElroy, T.P. Bui, R.J. Salawitch, S.S. Brown, A.R. Ravishankara, R.W. Portmann, M.K.W. Ko, D.K. Weisenstein, and P.A. Newman, 1999: A comparison of observations and model simulations of NO_x/NO_y in the lower stratosphere, *Geophys. Res. Lett.*, **26** (8), 1153 - 1156.

Hughes, L.S., J.O. Allen, P. Bhave, M.J. Kleeman, G.R. Cass, D.Y. Liu, D.F. Fergenson, B.D. Morrical, and K.A. Prather, 2000: Evolution of atmospheric particles along trajectories crossing the Los Angeles basin, *Environ. Sci. Technol.*, **34**, 3058-3068.

Kiselev, A.V., and V.I. Lygin, *Infrared Spectra of Surface Compounds*, John Wiley & Sons, Inc., New York, 1975.

Knipping, E.M., and D. Dabdub, 2002: Modeling surface-mediated 'renoxification' of the atmosphere via reaction of gaseous nitric oxide with deposited nitric acid, *Atmos. Environ.*, **in press**.

Lary, D.J., and D.E. Shallcross, 2000: Potential importance of the reaction $CO + HNO_3$, *J. Geophys. Res.*, **105** (D9), 11617-11623.

Low, M.J.D., and N. Ramasubramanian, 1966: Infrared study of the nature of the hydroxyl groups on the surface of porous glass, *J. Phys. Chem.*, **70** (9), 2740-2746.

McCurdy, P.R., P.W. Hess, and S.S. Xantheas, 2002: Nitric acid-water complexes: Theorethical calculations and comparison to experiment, *J. Phys. Chem. A*, **106**, 7628-7635.

Mochida, M., and B.J. Finlayson-Pitts, 2000: FTIR studies of the reaction of gaseous NO with HNO_3 on porous glass: Implications for conversion of HNO_3 to photochemically active NO_x in the atmosphere., *J. Phys. Chem. A*, **104** (43), 9705-9711.

Papirer, E., Adsorption on Silica Surfaces, in *Surfactant Science Series*, pp. 753, Marcel Dekker, Inc., New York, N. Y., 2000.

Perkins, K.K., T.F. Hanisco, R.C. Cohen, L.C. Koch, R.M. Stimpfle, P.B. Voss, G.P. Bonne, E.J. Lanzendorf, J.G. Anderson, P.O. Wennberg, R.S. Gao, L.A. Del Negro, R.J. Salawitch, C.T. McElroy, E.J. Hintsa, M. Loewenstein, and T.P. Bui, 2001: The NO_x-HNO_3 system in the lower stratosphere: Insights from *in situ* measurements and implications of the *J*HNO3-OH relationship, *J. Phys. Chem. A*, **105**, 1521 - 1534.

Portland Cement Association, Scientific Principles, Skokie, Illinois, 1999.

Rivera-Figueroa, A.M., A.L. Sumner, and B.J. Finlayson-Pitts, 2002: Laboratory studies of potential mechanism of renoxification of tropospheric nitric acid, *Environ. Sci. Technol.*, **submitted**.

Saliba, N., M. Mochida, and B.J. Finlayson-Pitts, 2000: Laboratory studies of sources of HONO in polluted urban atmospheres, *Geophys. Res. Lett.*, **27** (19), 3229-3232.

Saliba, N.A., H. Yang, and B.J. Finlayson-Pitts, 2001: Reaction of gaseous nitric oxide with nitric acid on silica surfaces in the presence of water at room temperature, *J. Phys. Chem. A*, **105** (45), 10339-10346.

Singh, H.B., W. Viezee, Y. Chen, A.N. Thakur, Y. Kondo, R.W. Talbot, G.L. Gregory, G.W. Sachse, D.R. Blake, J.D. Bradshaw, Y. Wang, and D.J. Jacob, 1998: Latitudinal distribution of reactive nitrogen in the free troposphere over the Pacific Ocean in late winter early spring, *J. Geophys. Res.*, **103** (D21), 28237-28246.

Staikova, M., and D.J. Donaldson, 2001: *Ab Initio* investigation of water complexes of some atmospherically important acids: HONO, HNO_3 and HO_2NO_2, *Phys. Chem. Chem. Phys.*, **3**, 1999-2006.

Tao, F.-M., K. Higgins, W. Klemperer, and D.D. Nelson, 1996: Structure, binding energy, and equilibrium constant of the nitric acid-water complex., *Geophys. Res. Lett.*, **23** (14), 1797-1800.

USGS, Sediment, U.S. Geological Survey, National Park Service, Department of Interior, Washington, DC, 1999.

WMO, Scientific Assessment of Ozone Depletion: 1998, World Meteorological Organization, Geneva, Switzerland, 1998.